Theoretical Investigation of the $O(^3P) + CHX_2$ (X = F, Cl) Reactions

Hua Hou, Baoshan Wang,* and Yueshu Gu

School of Chemistry, Shandong University, Jinan, Shandong 250100, P. R. China

Received: March 15, 1999; In Final Form: August 6, 1999

The reactions of oxygen atoms with the CHX_2 (X = F, Cl) radicals have been studied for the first time using the G2(MP2) method. The extensive calculations reveal the capture-limited association−elimination mechanism for the $O + CHX_2$ reaction. For the $O(^3P) + CHF_2$ reaction, two energy-rich intermediates, CHF_2O^* and CF_2OH^*, are formed along the reaction path. CHF_2O^* has four unimolecular production channels: $H + CF_2O$; CF_2OH; $F + CHFO$; and $HF + FCO$. The isomer CF_2OH can decompose to $H + CF_2O$, $HF + FCO$, $OH + CF_2$, and $F + FCOH$. The analogous production channels such as $Cl + CHClO$, $H + CCl_2O$, $HCl + ClCO$, $OH + CCl_2$, and $Cl + ClCOH$ are investigated for the $O(^3P) + CHCl_2$ reaction. It should be noted that three-center direct elimination of HCl from the adduct $CHCl_2O^*$ was characterized using the semiempirical AM1 method. On the basis of the ab initio potential energy surfaces, the kinetics and the dynamics for these two atom/radical reactions are discussed qualitatively. For the $O + CHF_2$ reaction, H and CF_2O are predicted to be the major products. For the $O(^3P) + CHCl_2$ reaction, the major production channel is the formation of $Cl + CHClO$, while the $HCl + ClCO$ channel may be competitive.

I. Introduction

The reactions of halogenated alkyl radicals with other highly reactive species have been of significant interest recently in atmospheric chemistry and in hydrocarbon combustion. Since hydrochlorofluorocarbons (HCFCs) have been widely used as replacements for chlorofluorocarbons (CFCs) in many industrial applications, the hydrogen abstraction of HCFCs by OH radical is believed to be one of the major sources of the halogenated alkyl radical.[1,2] The halogenated alkyl radicals can rapidly combine with atmospheric O_2 to form peroxy species, the subsequent reactions of which with NO produce vibrationally excited alkoxy radicals, which can play an important role in the degradation mechanism of other organic compounds.[3]

The reactions of halogenated alkyl radicals with atomic oxygen in the ^3P state are of special interest in combustion chemistry. High-temperature incineration is used as the primary means of disposal of large quantities of polymeric waste. Inevitably, a large number of halogenated alkyl radicals are generated through pyrolysis or complex chain reactions. Under fuel-lean conditions, the concentration of oxygen atoms is relatively high. Therefore, the atom/radical reaction of $O(^3P)$ with halogenated alkyl can occur to a significant extent.[4,5] Moreover, these reactions always involve many highly exothermic production channels that can contribute significantly over a wide range of temperatures.

We have initiated a series of studies of the reactions of $O(^3P)$ atoms with halogenated methyl CXYZ (X,Y,Z = H, F, Cl) radicals using ab initio molecular orbital (MO) theory to reveal their detailed mechanisms.[6] In this paper we report theoretical calculations for the $O(^3P) + CHX_2$ (X = F, Cl) reactions at the G2(MP2) level. Various possible reaction channels for these two reactions have been examined in detail, namely,

$$O(^3P) + CHF_2 \rightarrow HF + FCO + 465.3 \text{ kJ/mol}$$
$$\rightarrow H + CF_2O + 400.0 \text{ kJ/mol}$$
$$\rightarrow F + CHFO + 314.2 \text{ kJ/mol}$$
$$\rightarrow OH + CF_2 + 154.0 \text{ kJ/mol}$$

and

$$O(^3P) + CHCl_2 \rightarrow HCl + ClCO + 453.1 \text{ kJ/mol}$$
$$\rightarrow Cl + CHClO + 410.9 \text{ kJ/mol}$$
$$\rightarrow H + CCl_2O + 344.3 \text{ kJ/mol}$$
$$\rightarrow OH + CCl_2 + 71.5 \text{ kJ/mol}$$

where the reaction heats are estimated using experimental enthalpies of formation in the literature.[7−11] The overall kinetic and dynamic character of the $O + CHF_2$ and the $O + CHCl_2$ reactions is discussed on the basis of their ab initio potential energy surfaces. The dominant reaction channels are also predicted for the title reactions.

II. Computation Methods

Ab initio MO calculations were carried out using the Gaussian 94 programs.[12] The inexpensive and reliable G2(MP2) method[13] with some modifications was used to explore the lowest-lying doublet potential energy surfaces (PES) for the reactions of $O(^3P)$ with CHX_2 (X = F, Cl). The geometries of reactants, products, intermediates, and transition states were optimized at the UMP2=FU level. Because several important product channels involve C−H bond cleavage or hydrogen migration, the 6-31G(d,p) basis set, which adds one set of p functions to the hydrogen atom, was applied in the optimizations, rather than the standard 6-31G(d) basis set used in the original G2(MP2) scheme. The harmonic vibrational frequencies were obtained

* Corresponding author. E-mail: guojz@hosts.icm.sdu.edu.cn.

10.1021/jp990907n CCC: $18.00
Published on Web 09/18/1999

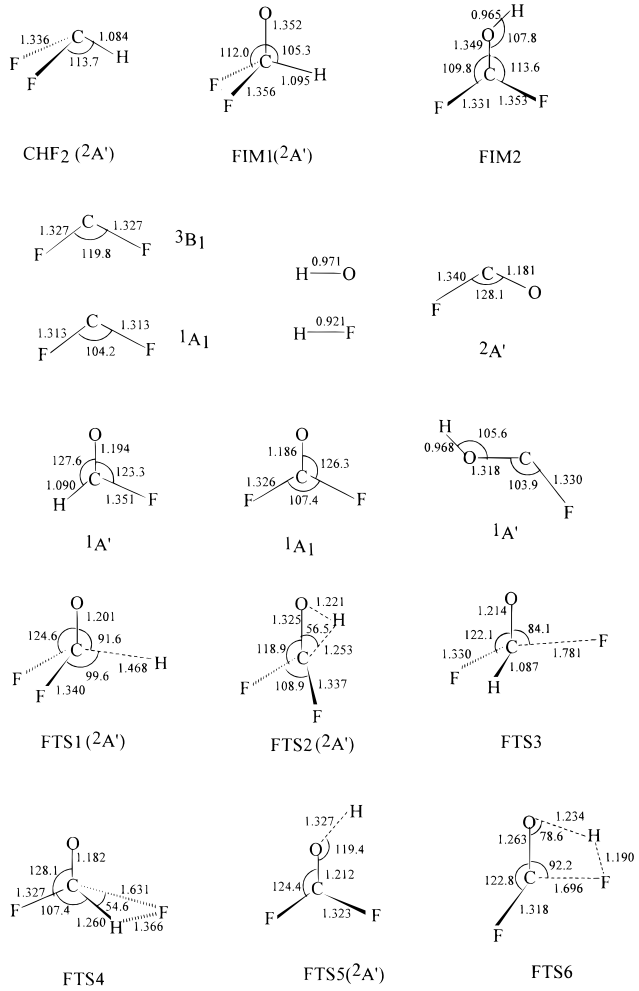

Figure 1. Optimized geometries at the UMP2=FU/6-31G(d,p) level for various species involved in the O + CHF_2 reaction.

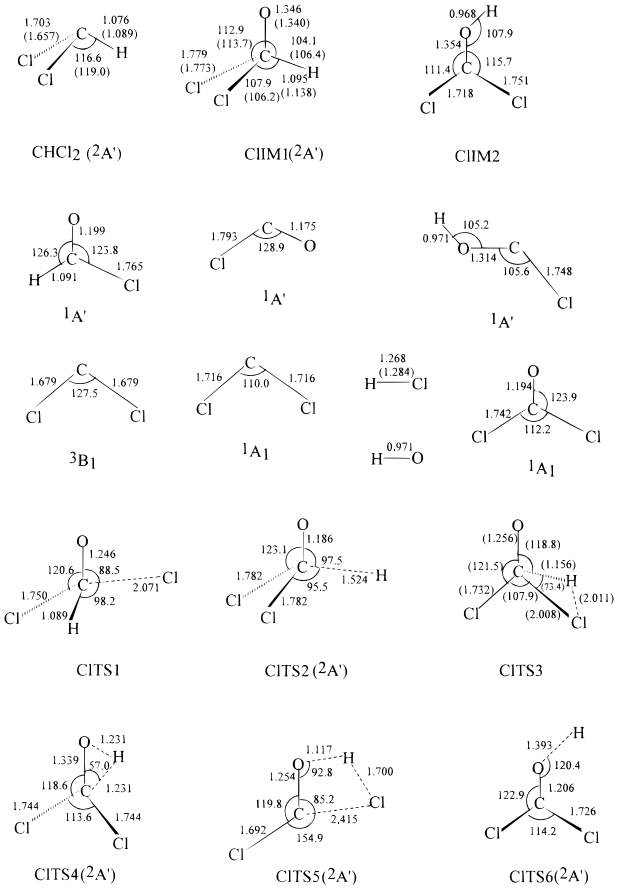

Figure 2. Optimized geometries at the UMP2=FU/6-31G(d,p) level for various species involved in the O + $CHCl_2$ reaction. The values in parentheses for $CHCl_2$, **ClIM1**, and **ClTS3** are the optimized geometric parameters at the AM1 level.

at the same level (UMP2=FU/6-31G(d,p) rather than the UHF/6-31G(d) level) in order to determine the nature of different stationary points as well as the zero-point energy (ZPE) corrections (scaled by a factor of 0.95 to partly eliminate the known systematic errors).[14] The number of imaginary frequency (0 or 1) confirms whether a local minimum or a transition state has been located. Connections of the transition states between designated reactants and products have been positively confirmed by intrinsic reaction coordinate (IRC) calculations[15] at the UMP2=FU/6-31G(d,p) level. Finally, the reliable energies for each species involved in the title reactions were calculated via the G2(MP2) protocol.

III. Results and Discussion

The optimized structures of various species involved in the reactions of O(^{3}P) + CHF_2 and O(^{3}P) + $CHCl_2$ are shown in Figures 1 and 2, and the vibrational frequencies are listed in Tables 1 and 2. The total energies and the relative energies are listed in Tables 3 and 4, respectively. To clarify the reaction mechanism, the profiles of the potential energy surfaces for the O(^{3}P) + CHF_2 and O(^{3}P) + $CHCl_2$ reactions are shown in Figures 3 and 4, respectively.

It is useful to compare the predicted thermochemistry with the experimental values. As can be seen from Tables 3 and 4, the calculated G2(MP2) reaction heats for various channels of the O + CHX_2 (X = F, Cl) reactions are in reasonable agreement with the experimental data except for three channels: the OH + CF_2 channel (−172.8 vs −154.0 kJ/mol) in the O(^{3}P) + CHF_2 reaction; the OH + CCl_2 channel (−85.7 vs −71.5 kJ/mol) in the O(^{3}P) + $CHCl_2$ reaction; the H + CCl_2O channel (−359.6 vs −344.3 kJ/mol) in the O(^{3}P) + $CHCl_2$ reaction. The calculated reaction exothermicity for these three channels at the G2(MP2) level significantly deviates from the experimental values. The unusually large deviation for this high level of calculation may be caused by the accumulation of the

TABLE 1: Scaled Vibrational Frequencies (in cm^{-1}) and Zero-Point Energies (ZPE, in kJ/mol) for Various Species Involved in the O + CHF_2 Reaction

species	frequency[a]	ZPE
CHF_2	515, 1039, 1146, 1174, 1341, 3076	49.6
CF_2O	547, 583, 732, 927, 1231, 1896	35.4
CHFO	630, 1004, 1066, 1360, 1794, 3050	53.3
FCOH	612, 790, 974, 1258, 1332, 3476	50.5
FCO	598, 1042, 1906	21.2
$CF_2(^1A_1)$	633, 1120, 1217	17.8
$CF_2(^3B_1)$	485, 1113, 1298	17.3
HF	3982	23.8
OH	3652	21.8
FIM1	440, 485, 618, 968, 1112, 1125, 1316, 1353, 2973	62.1
FIM2	273, 477, 481, 667, 1031, 1076, 1253, 1342, 3709	61.7
FTS1	1733i, 519, 521, 707, 773, 808, 1006, 1179, 1776	43.6
FTS2	2083i, 481, 499, 679, 694, 992, 1202, 1317, 2461	49.8
FTS3	1048i, 275, 405, 646, 1025, 1125, 1373, 1613, 3078	57.1
FTS4	620i, 371, 538, 681, 892, 1088, 1171, 1787, 2134	51.8
FTS5	2859i, 312, 526, 575, 595, 933, 962, 1267, 1794	41.6
FTS6	1681i, 266, 571, 695, 776, 884, 1139, 1563, 1978	47.1

[a] i represents imaginary frequency.

TABLE 2: Scaled Vibrational Frequencies (in cm^{-1}) and Zero-Point Energies (ZPE, in kJ/mol) for Various Species Involved in the $O + CHCl_2$ Reaction

species	frequency[a]	ZPE
$CHCl_2$	305, 529, 760, 900, 1257, 3168	41.4
	323, 379, 761, 990, 1094, 3020	*39.2*
CHClO	447, 735, 927, 1337, 1722, 3012	49.0
CCl_2O	304, 433, 562, 567, 846, 1756	26.7
ClCOH	447, 706, 733, 1238, 1269, 3614	47.9
ClCO	364, 616, 1900	17.2
$CCl_2(^1A_1)$	337, 732, 754	10.9
$CCl_2(^3B_1)$	300, 685, 988	11.8
HCl	2971	17.8
ClIM1	280, 315, 428, 668, 770, 1027, 1168, 1214, 2962	*52.8*
	276, 369, 446, 663, 775, 964, 1079, 1329, 2753	*51.8*
ClIM2	274, 328, 380, 466, 607, 834, 1176, 1258, 3663	53.8
ClTS1	837i, 206, 316, 445, 739, 930, 1306, 1338, 3037	49.7
ClTS2	1784i, 282, 391, 493, 598, 622, 701, 779, 1771	33.7
ClTS3	*842i, 214, 363, 385, 549, 779, 981, 1573, 2552*	*44.2*
ClTS4	2098i, 290, 372, 478, 613, 692, 847, 1195, 2503	41.8
ClTS5	1257i, 123, 180, 374, 580, 885, 988, 1476, 1834	38.5
ClTS6	2664i, 245, 306, 453, 466, 574, 800, 897, 1758	32.9

[a] The values in *italics* are calculated at AM1 level and scaled by a factor of 0.95. i represents imaginary frequency.

errors in the G2(MP2) total energies, which has been suggested in a few studies.[16]

1. Potential Energy Surface and Reaction Mechanism. *A. $O(^3P) + CHF_2$ Reaction.* The energetic profile (Figure 3) reveals an association−elimination mechanism for the $O(^3P) + CHF_2$ reaction. When $O(^3P)$ attacks the radical site of the CHF_2 radical, the reaction starts by the formation of an intermediate, CHF_2O^* (denoted as **FIM1**). As could be anticipated for the reactions of the radicals, no transition states are found along this addition path. The adduct **FIM1** has C_s symmetry and a $^2A'$ electronic state. The newly formed C−O bond is 1.352 Å. The other three bonds are somewhat longer than those of the CHF_2 radical. At the G2(MP2) level, the energy of **FIM1** is 414.8 kJ/mol lower than that of the reactants $O(^3P) + CHF_2$. It shows that **FIM1** should be a highly activated radical and thus may survive for a very short time. The rich internal energy of **FIM1** is available for subsequent dissociation or isomerization, which leads to various products. Four production channels of **FIM1** are found.

The energetically most favorable reaction path involves the formation of $H + CF_2O$ via the C−H bond cleavage transition state **FTS1**. The barrier height for this channel is calculated to be 61.6 kJ/mol at the G2(MP2) level. **FTS1** has C_s symmetry and a $^2A'$ electronic state. The breaking C−H bond is elongated from 1.095 Å in **FIM1** to 1.468 Å in **FTS1**. Meanwhile, the C−O bond is shortened by 0.151 Å. The geometrical parameters of the CF_2O group in **FTS1** are close to those of the final product CF_2O molecule. Thus, **FTS1** is a product-like barrier. This C−H bond fission channel of **FIM1** is slightly endothermic by 8.0 kJ/mol, while the overall reaction $O(^3P) + CHF_2 \rightarrow H + CF_2O$ is highly exothermic by 406.8 kJ/mol.

The second pathway involves the isomerization of **FIM1** to the CF_2OH radical (denoted as **FIM2**) via the 1,2-hydrogen shift, three-membered-ring transition state **FTS2**. The corresponding barrier height is 112.6 kJ/mol. **FTS2** has C_s symmetry and a $^2A'$ electronic state. The migrating hydrogen is 1.253 Å from the migrating origin (C) and 1.221 Å from the migrating terminus (O). The isomer **FIM2** has no symmetry. The newly formed O−H bond is 0.965 Å. The distances of the two C−F bonds are different by 0.02 Å. **FIM2** is 46.6 kJ/mol more stable than **FIM1** at the G2(MP2) level. Therefore, **FIM2** possesses higher internal energy than **FIM1**, and further, many decomposition channels of **FIM2** would be open as illustrated below.

The third reaction channel of **FIM1** produces F + CHFO via the C−F bond fission transition state **FTS3**. The breaking C−F bond is elongated by 0.425 Å and the C−O bond is shortened by 0.138 Å, while the O−C−F angle is reduced by 28.0°. The barrier height and the endothermicity for this channel are calculated to be 123.3 and 99.7 kJ/mol, respectively, while the overall reaction is highly exothermic by 315.1 kJ/mol.

The last examined reaction channel is the 1,1-HF elimination of **FIM1**, forming HF + FCO via the three-center transition state **FTS4**. The breaking C−H and C−F bonds are elongated simultaneously by 0.165 and 0.275 Å, respectively, with a decrease of the H−C−F angle to 54.6°. The forming H−F bond of 1.366 Å is 0.445 Å longer than the equilibrium distance of the HF molecule. The geometrical parameters of the FCO group in **FTS4** are almost equal to those of the final product FCO. The formation of HF + FCO has the highest barrier, 142.0 kJ/mol, among the four reaction channels of **FIM1** because of the strong repulsion of the three-membered ring. Moreover, it is also the most exothermic channel (by 466.2 kJ/mol) of the $O(^3P) + CHF_2$ reaction.

As mentioned above, the more energy-rich isomer **FIM2** can further decompose to various products. Five production channels of **FIM2** are found as follows.

The most feasible decomposition channel of **FIM2** is the formation of $H + CF_2O$ via the O−H bond fission transition state **FTS5** with a barrier of 134.4 kJ/mol. **FTS5** has C_s symmetry and a $^2A'$ electronic state. Two fluorine atoms are reflected by the HCO plane. The breaking O−H bond is elongated by 0.36 Å, while the C−O bond is shortened by 0.14 Å. It is noted that **FTS5** has a large imaginary frequency, 2859 cm^{-1}, which may indicate a narrow barrier and thus large tunneling.

The second reaction channel of **FIM2** is the 1,2-HF elimination leading to HF + FCO via transition state **FTS6**. The four-membered ring FCOH is nearly planar. The breaking C−F and O−H bonds are 1.696 and 1.234 Å, respectively. The forming H−F bond of 1.190 Å is 0.27 Å longer than the equilibrium distance of the HF molecule. The barrier height is 180.7 kJ/mol relative to **FIM2**. It is interesting to note that two different transition states, three-center **FTS4** and four-center **FTS6**, which lead to the same products HF + FCO, happen to have similar energies.

The last three production channels of **FIM2** are all simple bond fission processes without any barriers. The C−O and C−F bond fissions of **FIM2** produce $OH + CF_2$ ($^1A_1$) and F + FCOH with endothermicities of 288.6 and 324.2 kJ/mol, respectively. But for the overall $O(^3P) + CHF_2$ reaction, both $OH + CF_2$ and F + FCOH products are still energetically accessible. However, if the CF_2 radical is formed in the triplet state, the overall reaction $O + CHF_2 \rightarrow OH + CF_2(^3B_1)$ is no longer energetically accessible because of its endothermicity of 75.6 kJ/mol.

B. $O(^3P) + CHCl_2$ Reaction. Similar to the $O(^3P) + CHF_2$ reaction, the $O(^3P) + CHCl_2$ reaction also involves an association−elimination mechanism, as indicated in Figure 4. $O(^3P) + CHCl_2$ react on a strongly attractive potential energy surface, forming an intermediate $CHCl_2O^*$ (denoted as **ClIM1**). The adduct **ClIM1** has C_s symmetry and a $^2A'$ electronic state. The newly formed C−O bond is 1.346 Å. The exothermicity of **ClIM1** formation at the first reaction step is calculated to be 367.7 kJ/mol at the G2(MP2) level. It is obvious that **ClIM1** is an energy-rich radical with a short lifetime. Four reaction channels of **ClIM1** are examined.

TABLE 3: Total Energies (in hartree) at Various Levels and the Relative Energies Δ*E* (in kJ/mol) at the G2(MP2) Level for Various Species Involved in the O + CHF_2 Reaction

species	QCISD(T) /6-311G(d,p)	UMP2 /6-311G(d,p)	UMP2 /6-311+G(3df,2p)	G2(MP2)	Δ*E*	exptl relative energy[a]
O + CHF_2	−312.815 47	−312.773 52	−312.948 95	−313.027 58	0.0	
HF + FCO	−312.975 70	−312.945 42	−313.131 83	−313.205 15	−466.2	−465.3 ± 7.1
H + CF_2O	−312.951 15	−312.928 28	−313.112 93	−313.182 52	−406.8	−400.0 ± 8.4
F + CHFO	−312.931 05	−312.895 35	−313.072 00	−313.147 61	−315.1	−314.2 ± 11.7
OH + $^1CF_2$	−312.865 08	−312.821 26	−313.004 48	−313.093 40	−172.8	−154.0 ± 13.8
OH + $^3CF_2$	−312.777 42	−312.738 30	−312.919 02	−312.998 78	75.6	
F + FCOH	−312.860 10	−312.817 91	−312.994 06	−313.079 84	−137.2	
FIM1	−312.963 86	−312.925 62	−313.110 82	−313.185 58	−414.8	
FIM2	−312.977 39	−312.946 95	−313.137 25	−313.203 32	−461.4	
FTS1	−312.930 60	−312.891 98	−313.079 89	−313.162 10	−353.2	
FTS2	−312.912 07	−312.876 58	−313.066 00	−313.142 71	−302.2	
FTS3	−312.915 94	−312.864 63	−313.048 84	−313.138 60	−291.5	
FTS4	−312.903 58	−312.866 81	−313.054 28	−313.131 50	−272.8	
FTS5	−312.918 87	−312.880 04	−313.068 97	−313.152 13	−327.0	
FTS6	−312.904 29	−312.875 08	−313.063 04	−313.134 51	−280.7	

[a] Calculated using the reported experimental enthalpies of formation in refs 7, 8, 10, and 11.

TABLE 4: Total Energies (in hartree) at Various Levels and the Relative Energies Δ*E* (in kJ/mol) at the G2(MP2) Level for Various Species Involved in the O + $CHCl_2$ Reaction

species[a]	QCISD(T) /6-311G(d,p)	UMP2 /6-311G(d,p)	UMP2/6-311+G(3df,2p)	G2MP2	Δ*E*	exptl relative energy[b]
O + $CHCl_2$	−1 032.796 08	−1 032.731 99	−1 032.902 69	−1 033.006 59	0.0	
O + $CHCl_2$	*−1 032.792 43*	*−1 032.728 98*	*−1 032.900 98*	*−1 033.005 03*	*0.0*	
HCl + ClCO	−1 032.958 74	−1 032.904 63	−1 033.082 11	−1 033.183 09	−463.4	−453.1 ± 12.6
Cl + CHClO	−1 032.946 87	−1 032.893 57	−1 033.068 93	−1 033.163 39	−411.7	−410.9 ± 14.6
H + CCl_2O	−1 032.909 26	−1 032.865 04	−1 033.049 31	−1 033.143 54	−359.6	−344.3 ± 16.7
Cl + ClCOH	−1 032.872 03	−1 032.811 39	−1 032.987 70	−1 033.090 30	−219.8	
OH + $^1CCl_2$	−1 032.807 28	−1 032.739 48	−1 032.923 71	−1 033.039 22	−85.7	−71.5 ± 18.0
OH + $^3CCl_2$	−1 032.779 33	−1 032.716 31	−1 032.895 25	−1 033.001 02	14.6	
ClIM1	−1 032.924 73	−1 032.864 74	−1 033.046 58	−1 033.146 64	−367.7	
ClIM1	*−1 032.923 58*	*−1 032.863 38*	*−1 033.045 53*	*−1 033.146 20*	*−370.6*	
ClIM2	−1 032.943 40	−1 032.891 11	−1 033.078 53	−1 033.170 52	−430.4	
ClTS1	−1 032.917 81	−1 032.848 62	−1 033.032 75	−1 033.143 18	−358.6	
ClTS2	−1 032.889 53	−1 032.827 78	−1 033.014 89	−1 033.123 99	−308.2	
ClTS3	*−1 032.906 97*	*−1 032.834 84*	*−1 033.018 16*	*−1 033.133 63*	*−337.6*	
ClTS4	−1 032.877 26	−1 032.820 37	−1 033.006 78	−1 033.107 94	−266.1	
ClTS5	−1 032.891 94	−1 032.836 74	−1 033.020 37	−1 033.121 09	−300.6	
ClTS6	−1 032.884 88	−1 032.824 31	−1 033.011 91	−1 033.120 14	−298.2	

[a] The values in *Italics* are calculated using the AM1-optimized geometries. [b] Calculated using the reported experimental enthalpies of formation in refs 9−11.

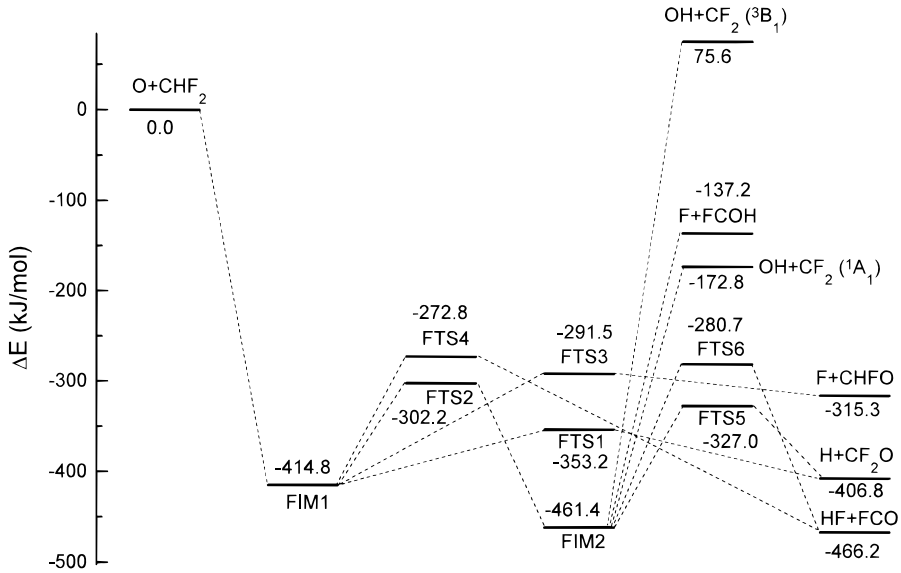

Figure 3. Energetic profile for the potential energy surface of the O + CHF_2 reaction at the G2(MP2) level.

The energetically favorable decomposition path of **ClIM1** is C−Cl bond cleavage via a very low barrier, **ClTS1**. The barrier height is only 9.1 kJ/mol at the G2(MP2) level. It implies that the formation of the $CHCl_2O$ radical and its subsequent Cl-atom extrusion is almost concerted. This mechanism is different from that for the C−F bond cleavage of the CHF_2O radical,

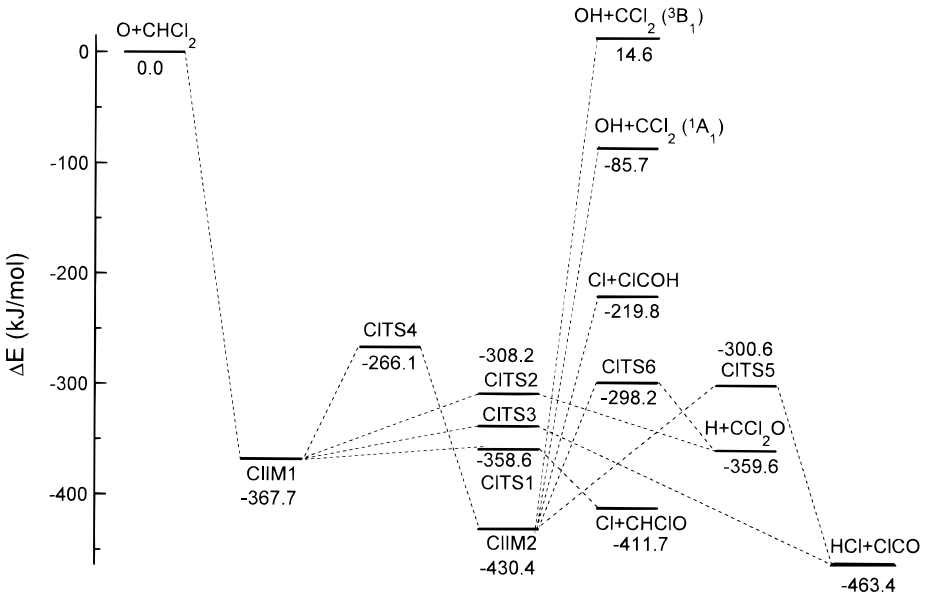

Figure 4. Energetic profile for the potential energy surface of the O + $CHCl_2$ reaction at the G2(MP2) level.

which involves a much higher barrier. The breaking C−Cl bond is stretched to 2.071 Å, and the O−C−Cl angle decreases from 112.9° in **ClIM1** to 88.5° in **ClTS1**. The C−O bond is shortened by 0.1 Å in forming the final product CHClO. This channel is exothermic by 44.0 kJ/mol.

The second decomposition path of **ClIM1** produces H + CCl_2O via the C−H bond fission transition state **ClTS2**. The barrier height for this step, 59.5 kJ/mol, is similar to that for the C−H bond fission of **FIM1** in the $O(^3P) + CHF_2$ reaction. **ClTS2** has C_s symmetry and a $^2A'$ electronic state. **ClTS2** has a product-like geometry. The breaking C−H bond is elongated by 0.429 Å, and the C−O bond is shortened by 0.16 Å. This channel is slightly endothermic by 8.1 kJ/mol, while the overall reaction is highly exothermic by 359.6 kJ/mol.

It is noteworthy that both C−Cl and C−H bonds in the $CHCl_2O$ radical are relatively weak. The corresponding decomposition barriers are 9.1 and 59.5 kJ/mol, respectively. Meanwhile, the production of HCl + ClCO is the most exothermic channel in the $O(^3P) + CHCl_2$ reaction. The exothermicity is 95.7 kJ/mol relative to that of **ClIM1**. Therefore, the direct three-center intramolecular elimination of HCl from **ClIM1** should be a favorable channel. As a matter of fact, three-center HCl elimination from the analogous alkoxy radicals (e.g., CH_2ClO[6,17−19] and CH_3CHClO[20−22]) has been characterized experimentally and theoretically.

For the three-center elimination of HCl from **ClIM1**, we can only find the corresponding transition state at the semiempirical AM1 level. The optimized structure is shown as **ClTS3** in Figure 2. To determine the reliability of this semiempirical structure, we have calculated the geometries, vibrational frequencies, and ZPE for the reactants $O(^3P) + CHCl_2$ and the **ClIM1** adduct using the AM1 method. Moreover, high-level energies were also calculated using the G2(MP2) scheme on the basis of the AM1-optimized geometries. The results are also listed in Figure 2, Table 2, and Table 4, respectively, for the purpose of comparison. By use of the G2(MP2) scheme, the exothermicity of **ClIM1** is 367.7 kJ/mol based on the UMP2=FU/6-31G(d,p) optimized geometries, and 370.6 kJ/mol based on the AM1 optimized geometries. The energy difference, 2.9 kJ/mol, implies that the AM1 method should be reliable, at least qualitatively. So the AM1-optimized **ClTS3** structure may be valid.

As can be seen in Figure 2, **ClTS3** is a rather early barrier. The C−H bond is stretched very slightly and the C−Cl bond is elongated by ∼0.24 Å, while the H−C−Cl angle decreases by ∼33°. The forming HCl bond distance of 2.011 Å is ∼0.73 Å longer than the equilibrium value of the free HCl molecule. These structural characteristics are analogous to those of the transition state for HCl elimination from the CH_2ClO radical.[6] At the G2(MP2) level, the barrier height is 33.0 kJ/mol, which is 24.0 kJ/mol higher than **ClTS1** for the C−Cl bond cleavage. This is different from the decomposition of the CH_2ClO radical, where the HCl elimination possesses the lowest barrier and thus is the most favorable decomposition channel.[6]

The fourth reaction channel involves the isomerization of **ClIM1** via the three-membered-ring transition state **ClTS4** with 1,2-hydrogen shift, forming the intermediate CCl_2OH (denoted as **ClIM2**). The breaking C−H bond and forming O−H bond have the same distances, 1.231 Å. The barrier height is calculated to be 101.6 kJ/mol. The energy of **ClIM2** is 62.7 kJ/mol lower than that of **ClIM1**. **ClTS4** has C_s symmetry, while the isomer **ClIM2** has no symmetry. One of the chlorines in **ClIM2** is nearly in the HOC plane.

Because the intermediate **ClIM2** possesses rich internal energy (430.4 kJ/mol relative to those of the reactants $O(^3P)$ + $CHCl_2$), it can further decompose to various products.

The first feasible decomposition channel of **ClIM2** is the formation of HCl + ClCO via the 1,2-HCl elimination four-center transition state **ClTS5**. Different from the transition state **FTS6** for the HF elimination of **FIM2**, **ClTS5** has C_s symmetry and a $^2A'$ electronic state. The breaking C−Cl and O−H bonds are stretched simultaneously to 2.415 and 1.117 Å, respectively. The forming H−Cl bond is 1.70 Å, 0.432 Å longer than the equilibrium distance of the HCl molecule. The corresponding barrier height is 129.8 kJ/mol relative to **ClIM2**.

The O−H bond cleavage of **ClIM2** produces H + CCl_2O via transition state **ClTS6**, which is nearly equal in energy to **ClTS5**. The breaking O−H bond is elongated by 0.425 Å. **ClTS6** has a large imaginary frequency, 2664 cm^{-1}.

The last three decomposition paths of **ClIM2** are all simple bond fissions. The C−Cl and C−O fissions produce Cl + ClCOH and OH + CCl_2, with endothermicities of 210.6 and 344.7 kJ/mol, respectively. The formation of the OH + CCl_2-

($^3B_1$) radicals is not energetically favorable because of an overall endothermicity of 14.6 kJ/mol.

2. Kinetic and Dynamic Analysis. *A. Kinetics of the Overall Reaction.* As can be seen from the energetic profiles (Figures 3 and 4), both **FIM1** and **ClIM1** correspond to deep potential wells on the PES relative to the entrances of the $O(^3P) + CHF_2$ and $O(^3P) + CHCl_2$ reactions. Obviously, it is difficult for **FIM1** and **ClIM1** to redissociate back to the reactants. On the other hand, the subsequent decomposition or isomerization reactions of **FIM1** and **ClIM1** occur with relatively low exit barriers. Therefore, both the $O + CHF_2$ and the $O + CHCl_2$ reactions should be capture-limited; i.e., the barrierless association process is the rate-determining step with the near gas collision number rate $\sim 10^{-10}$ cm^3 molecule^{-1} s^{-1}. Furthermore, the rate constant would exhibit a negative temperature dependence, which is typical for atom/radical reactions because the initial association is barrier-free and because the exit barriers lie well below the energy available to the system. Meanwhile, the rate constants for the title reactions should be pressure-independent because the lifetime of the initial adduct is too short to be deactivated effectively through collisions with the bath gases. Similar kinetic behavior has been observed experimentally in several analogous reactions such as $O(^3P) + CH_2Cl$[4] and $O(^3P) + CCl_3$.[5]

B. Dynamics and Yields. In principle, the yields of various products in the $O(^3P) + CHX_2$ (X = F, Cl) reactions can be estimated by the rates for the various unimolecular decomposition channels of CHX_2O^* using RRKM theory:[23]

$$k_i(E) = l_i \left(\frac{I_i^{\ddagger}}{I}\right)^{1/2} \frac{G_i(E-E_i^{\ddagger})}{hN(E)}$$

where l_i is the reaction path degeneracy and h is Planck's constant. $N(E)$ is the density of states of CHX_2O^* at energy E, $G_i(E-E_i^{\ddagger})$ is the sum of states of the transition state for channel i at $E - E_i^{\ddagger}$, and $E_i^{\ddagger}$ is the corresponding barrier height. The vibrational frequencies and the moments of inertia for CHX_2O^* and the various transition states are taken from the present ab initio calculations.

However, it is worthwhile noting that the energy-specific rate constants, $k_i(E)$, are quite large, for example, $10^{13}-10^{14}$ s^{-1} at $E = E_R$ (E_R is the energy of the reactants relative to CHX_2O), because of the high internal energy of CHX_2O^* and its low exit barriers. This means that the lifetime of the CHX_2O^* radical lies in the range $10^{-14}-10^{-13}$ s, which is too short, in general, to allow energy randomization and a statistical distribution of the available energy among the accessible product states. Even though there exists a strongly bound intermediate in the atom/radical reaction, it must have little effect on the dynamics, which is thus similar to those taking place in a direct process. As a result, the polyatomic products, such as HF, HCl, CF_2O, CCl_2O, CHFO, CHClO, etc., should be internally excited with a strongly nonstatistical vibrational distribution as observed in the $O + C_2H_3$ reaction.[24] So the statistical RRKM calculation is no longer suitable rigorously. The yields of the products should be determined only by the corresponding barrier heights.

For the $O(^3P) + CHF_2$ reaction, as can be seen in Figure 3, the formation of $H + CF_2O$ from CHF_2O^* possesses the lowest barrier, 61.6 kJ/mol. Furthermore, the decomposition of the isomer CF_2OH^* to $H + CF_2O$ also involves its lower barrier. So the major products of the $O + CHF_2O$ reaction should be $H + CF_2O$.

For the $O(^3P) + CHCl_2$ reaction, as shown in Figure 4, the Cl-atom extrusion from the $CHCl_2O$ radical has a very low barrier of 9.1 kJ/mol. The HCl elimination channel possesses a barrier of 33.0 kJ/mol. As mentioned above, although a large uncertainty for the barrier height of this three-center HCl elimination channel may be introduced because the transition state **ClTS3** can be characterized only at the AM1 semiempirical level, the difference of ~24.0 kJ/mol between **ClTS1** and **ClTS3** is so large that a qualitative conclusion can be drawn: the $O(^3P) + CHCl_2$ reaction will produce Cl + CHClO dominantly, while the production of HCl + ClCO is a competitive channel at most.

IV. Concluding Remarks

The G2(MP2) calculations reveal a capture-limited association−elimination mechanism for both $O + CHF_2$ and $O + CHCl_2$ reactions. High-quality ab initio potential energy surfaces are reported. Various possible intermediates and transition states were located along the reaction paths. The title reactions show unique kinetic and dynamic behavior. It is predicted that H and CF_2O are the major products in the $O + CHF_2$ reaction. The formation of Cl + CHClO probably dominates the $O + CHCl_2$ reaction, but the formation of HCl + ClCO may be competitive.

Acknowledgment. We thank two referees for their careful and valuable comments, especially suggesting the possible existence of **ClTS3**, which we failed to find initially.

References and Notes

(1) Atkinson, R. J. *J. Phys. Chem. Ref. Data, Monogr. 1* **1989**.

(2) Fang, T. D.; Taylor, P. H.; Dellinger, B.; Ehlers, C. J.; Berry, R. J. *J. Phys. Chem. A* **1997**, *101*, 5758.

(3) Wallingtom, T. J.; Hurley, M. D.; Fracheboud, J. M.; Orlando, J. J.; Tyndall, G. S.; Sehested, J.; Mogelberg, T. E.; Nielson, O. J. *J. Phys. Chem.* **1996**, *100*, 18116.

(4) Seetula, J. A.; Slagle, I. R. *Chem. Phys. Lett.* **1997**, *277*, 381.

(5) Seetula, J. A.; Slagle, I. R.; Gutman, D.; Senkan, S. M. *Chem. Phys. Lett.* **1996**, *252*, 299.

(6) Wang, B.; Hou, H.; Gu, Y. *J. Phys. Chem. A* **1999**, *103*, 2060. In this paper, the lost transition state for the three-center elimination of HCl from CH_2ClO (**IM1**) is now found at various levels of theory (e.g., UMP2/6-31G(d,p), UB3LYP/6-31G(d), UB3LYP/6-311G(d,p), etc.). The calculations show that the HCl elimination channel possesses the lowest barrier, 45.6 kJ/mol at the G2(MP2) level. So our previous prediction of the major products in the $O(^3P) + CH_2Cl$ reaction is not valid. The major products should be HCl + ClCO rather than Cl + CH_2O. Other conclusions in this paper are still correct. The optimized geometries, vibration frequencies, IRC data, and energies for this three-center transition state can be obtained by email (guojz@hosts.icm.sdu.edu.cn).

(7) Poutsma, J. C.; Paulino, J. A.; Squires, R. R. *J. Phys. Chem. A* **1997**, *101*, 5327.

(8) Dixon, D. A.; Feller, D. *J. Phys. Chem. A* **1998**, *102*, 8209.

(9) Rodriquez, C. F.; Bohme, D. K.; Hopkinson, A. C. *J. Phys. Chem.* **1996**, *100*, 2942.

(10) Curtiss, L. A.; Raghavachari, K.; Redfern, P. C.; Pople, J. A. *J. Chem. Phys.* **1997**, *106*, 1063.

(11) Demore, W. B.; Sander, S. P.; Golden, D. M.; Hampson, R. F.; Kurylo, M. J.; Howard, C. J.; Ravishankara, A. R.; Kolb, C. E.; Molina, M. J. *Chemical Kinetics and Photochemical Data for Use in Stratospheric Modeling*; Evaluation Number 12; Jet Propulsion Laboratory: Pasedena, CA, 1997.

(12) Frisch, M. J.; Trucks, G. W.; Schlegel, H. B.; Gill, P. W. M.; Johnson, B. G.; Robb, M. A.; Cheeseman, J. R.; Keith, T. A.; Petersson, G. A.; Montgomery, J. A.; Raghavachari, K.; Allaham, M. A.; Zakrzewski, V. G.; Ortiz, J. V.; Foresman, J. B.; Cioslowski, J.; Stefanov, B. B.; Nanayakkara, A.; Challacombe, M.; Peng, C. Y.; Ayala, P. Y.; Chen, W.; Wong, M. W.; Andres, J. L.; Replogle, E. S.; Gomperts, R.; Martin, R. L.; Fox, D. J.; Binkley, J. S.; Defrees, D. J.; Baker, J.; Stewart, J. P.; Head-Gordon, M.; Gonzales, C.; Pople, J. A. *Gaussian 94*; Gaussian Inc.: Pittsburgh, PA, 1995.

(13) Curtiss, L. A.; Ragharachari, K.; Pople, J. A. *J. Chem. Phys.* **1993**, *98*, 1293.

(14) Hehre, W. J.; Radom, L.; Schleyer, P. V. R.; Pople, J. A. *Ab initio Molecular Orbital Theory*; John Wiley: New York, 1986.

(15) Gonzalez, C.; Schlegal, H. B. *J. Chem. Phys.* **1989**, *90*, 2154.

(16) Mebel, A. M.; Diau, E. W. G.; Lin, M. C.; Morokuma, K. *J. Am. Chem. Soc.* **1996**, *118*, 9759.

(17) Catoire, V.; Lesclaux, R.; Lightfoot, P. D.; Rayez, M. T. *J. Phys. Chem.* **1994**, *98*, 2889.

(18) Kaiser, E. W.; Wallington, T. J. *J. Phys. Chem.* **1994**, *98*, 5679.

(19) Wallington, T. J.; Orlando, J. J.; Tyndall, G. S. *J. Phys. Chem.* **1995**, *99*, 9437.
(20) Shi, J.; Wallington, T. J.; Kaiser, E. W. *J. Phys. Chem.* **1993**, *97*, 6184.
(21) Maricq, M. M.; Shi, J.; Szente, J. J.; Rimai, J.; Kaiser, E. W. *J. Phys. Chem.* **1993**, *97*, 9686.
(22) Kaiser, E. W.; Wallington, T. J. *J. Phys. Chem.* **1995**, *99*, 8669.
(23) Forst, W. *Theory of Unimolecular Reactions*; Academic Press: New York, 1973.
(24) Donaldson, D. J.; Okuda, I. V.; Sloan, J. J. *Chem. Phys.* **1995**, *193*, 37.